# Energy-Deposition Events Measured by the CRRES PHA Experiment

P. J. McNulty, J. D. Kinnison, R. H. Maurer, D. R. Roth, R. A. Reed, and W. G. Abdel-Kader

***Abstract*—The energy-deposition spectra measured by the CRRES (Combined Release and Radiation Effects Satellite) pulse height analyzer (PHA) experiment are reexamined to determine the relative contributions from the different mechanisms by which large localized energy-deposition events can be generated in silicon detector volumes flown in space. Comparisons with calculations generated by the CUPID simulation model modified to include pion-production and elastic-scattering events are used to generate a "best fit" trapped proton spectrum that is compared to the predictions of the NASA models for the CRRES orbit.**

***Index Terms*—Dosimetry, protons, radiation effects, radiation monitoring.**

## I. Introduction

WHEN exposed to a beam of energetic charged particles, a solid-state detector measures a distribution of pulse heights, each proportional to the energy deposited within the sensitive volume of the detector. If the sensitive volume of the detector is sufficiently large that all the energy from the incident charged particle is collected, the measured energy-deposition spectrum is identical to the incident spectrum of the particles. At high incident energies, however, collection of the total incident energy is not practical. Only the energy loss generated in the detector by the incident charged particle and the energy loss from the secondary charged particles emerging from any nuclear reactions contribute to the measured pulse-height event. Elastic nuclear reactions and spallation reactions dominate the large energy-deposition events because of the high linear energy transfer (LET) and short range of the recoiling nucleus or nuclear fragment. This so-called effective LET spectrum can be obtained from pulse-height measurements obtained from simple silicon solid-state detectors, photodiodes, or arrays of p–n microjunctions. These detectors are rugged, inexpensive, and lightweight instruments [1], [2] that require little power and provide data in a form suitable for comparison with the environmental models combined with available interaction models such as CUPID [3]. Energy spectra are superior to LET spectra for studying the space environment and managing radiation effects, but for high-energy protons, the practicality of either collecting all the incident particle's energy or developing an accurate time-of-flight system precludes flux measurements at high energies in small efficient instruments.

This paper determines the relative contributions from the elastic-scattering events, pion-production events, and direct hits by cosmic rays and grazing low-energy protons from the pulse-height spectrum measured with a simple silicon detector. The method is demonstrated on data obtained from the pulse height analyzer (PHA) instrument flown as part of the Microlectronics Package Experiment on the CRRES (Combined Release and Radiation Effects Satellite). In recent years, a simple algorithm for obtaining the primary particle energy spectrum from pulse-height measurements generated by thick solid-state detectors has been developed [4] and shown to provide good agreement with established models of the energy spectrum of the Los Alamos National Laboratory neutron source [5]. A full description of the methodology is given in [4] and [6]. Since protons and neutrons undergo similar interactions at high energies, the technique should also be applicable to thin detectors in high-energy proton environments provided that the response of the detector to monoenergetic protons can be determined by experiment or modeling. This response-function method is used in this study to determine the incident-energy spectrum of high-energy protons trapped in the Earth's inner radiation belt from the data measured with a small photodiode, the UV100.

The objective of the study was to determine the relative contributions to the measured spectra from elastic-scattering events, spallation events, pion-production events, and cosmic-ray events, and, in particular, to determine the contribution, if any, from low-energy protons incident on the detector at grazing angles. Modern photonic systems have sensors that have extremely low thresholds for single-event upset (SEU), making low energy-deposition events in large silicon volumes important. On the other hand, SEUs in some other technologies have very high thresholds making it important to be able to predict the entire spectrum of energy depositions to be expected on spacecraft.

## II. Background

At the time this project began, the CUPID codes were known to give reasonably good agreement with the experimental data, especially for incident energies below 200 MeV and large energy depositions, the type of events that initiate SEU events in microelectronics [3]. This is shown clearly in Fig. 1 where the agreement between theory and experiment is quite close for incident energies up to 200 MeV, and even then the disagreement

Manuscript received 22 July, 2004. This work was supported in part by the Marshall Space Flight Center under NAG8-1695 and by NASA's Living With a Star/Space Environments Testbeds under Project 2092903.

P. J. McNulty is with the Department of Physics, Clemson University, Clemson, SC 29634-0978 USA (e-mail: mpeter@clemson.edu).

J. D. Kinnison is with the Applied Physics Laboratory, Johns Hopkins University, Laurel, MD 20723-6099 USA and also with Clemson University, Clemson, SC 29117 USA (e-mail: jim.kinnison@jhuapl.edu).

R. H. Maurer and D. R. Roth are with the Applied Physics Laboratory, Johns Hopkins University, Laurel, MD 20723-6099 USA.

R. A. Reed is with the NASA Goddard Space Flight Center, Greenbelt, MD 20771 USA (e-mail: Robert.Reed@gsfc.nasa.gov).

W. G. Abdel-Kader is with the South Carolina State University, Orangeburg, SC 29117 USA (e-mail: abdelkaderwg@ scsu.edu).

Digital Object Identifier 10.1109/TNS.2004.839241

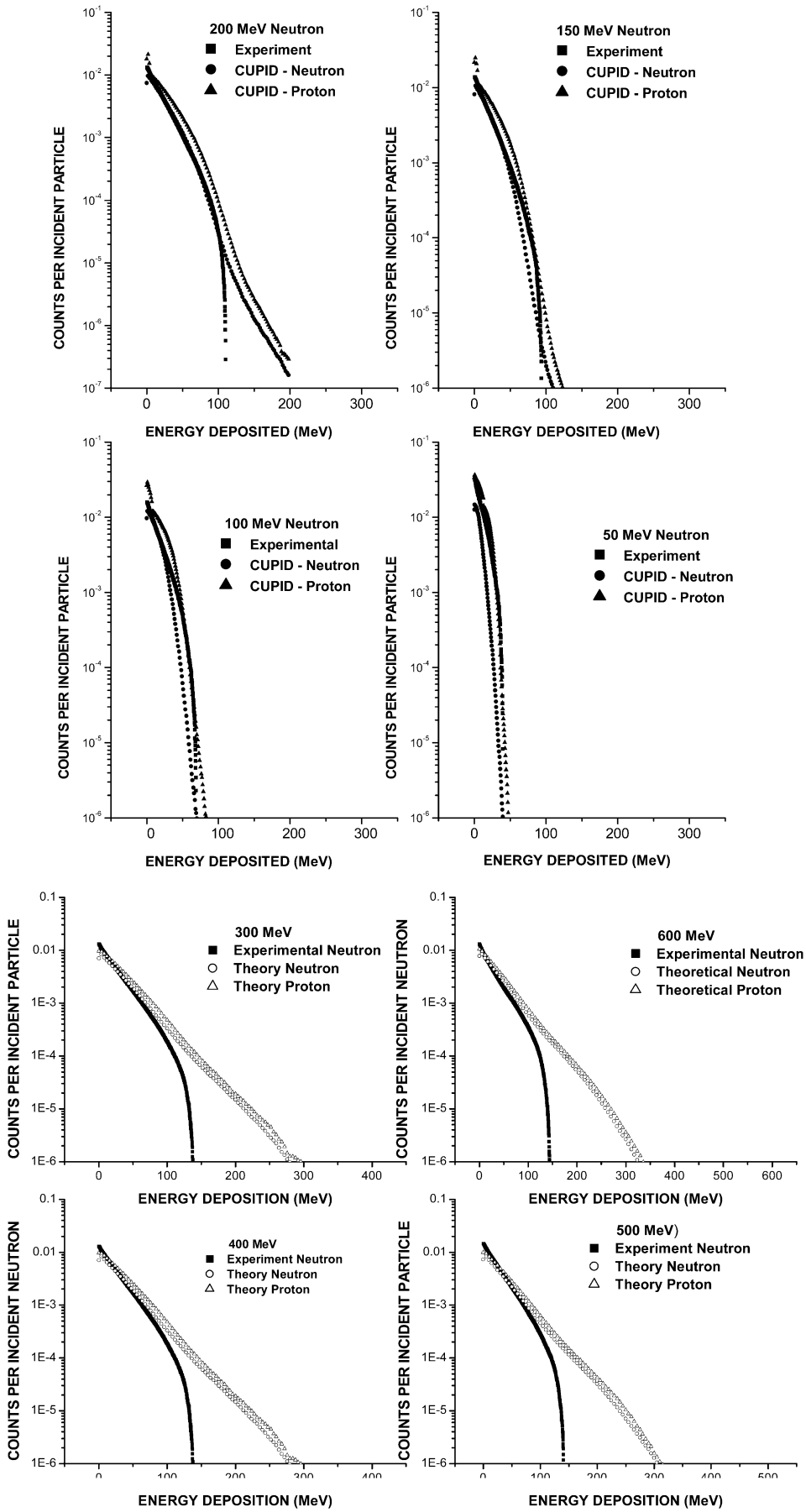


Fig. 1. Integral pulse-height spectra generated within an Ortec Li-drifted silicon solid-state detector by neutrons of different incident energies. The sensitive volume was cylindrical with 2 $cm^2$ area and 0.5 cm thickness.

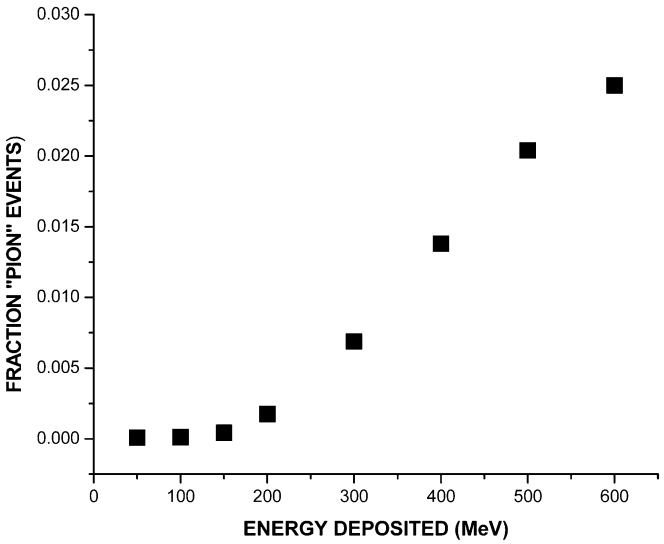


Fig. 2. The fraction of all spallation events in which a pion is produced, as calculated by the modified version of CUPID. Since it takes 140 MeV to create the rest mass of the pion in the center of momentum frame of reference, pions are not generated in significant numbers until incident energies of about 200 MeV.

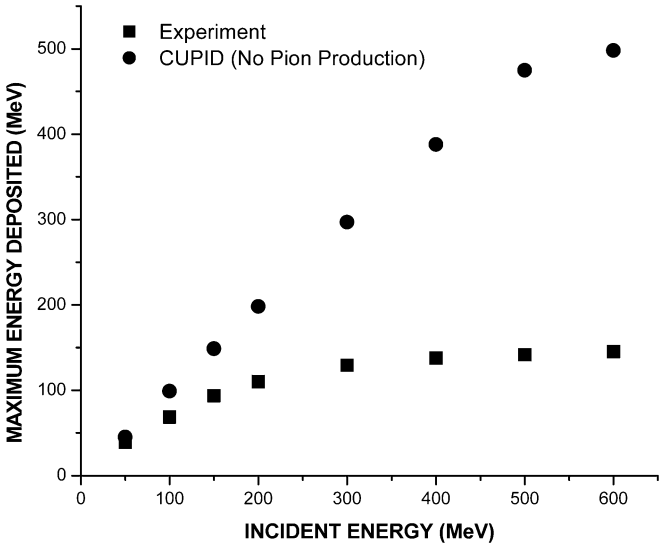


Fig. 3. Maximum energy deposited within an Si solid-state detector with a cylindrical volume of 2 $cm^2 \times 0.5$ cm. The removal of energy from the detector by the pion increases with the incident energy of the neutron.

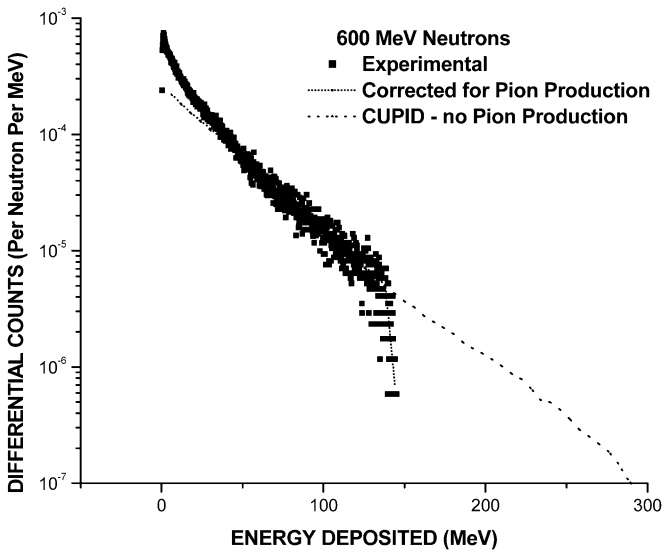


Fig. 4. Differential event cross section versus the energy deposited in the Ortec Si Li-drifted detector. Comparison is made with CUPID simulations with and without pion production. The significant difference between theory and experiment at low energy depositions is due to elastic-scattering events.

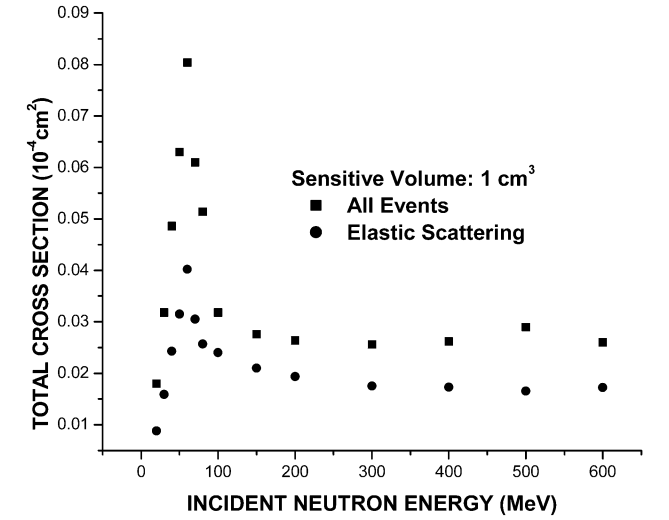


Fig. 5. Total device cross section for depositing more than 13.4 MeV in the Ortec Silicon Li-drifted solid-state detector compared to the elastic-scattering event cross section obtained from the difference between the measured cross section and the value calculated by the pion-producing version of CUPID.

represents only the highest 1% of energy depositions. By incident energies of 600 MeV, pion production still only removes energy from the highest 10% of predicted energy depositions. This small disagreement was shown to be due to events in which pions are produced that remove large amounts of energy from the localized energy-deposition event [6]. The fraction of all spallation events that involve production of a pion is plotted versus the incident proton energy in Fig. 2.

Despite the small number of pion-producing events, they strictly limit the production of large energy-deposition events as shown in Fig. 3 which compares the maximum energy deposited according to CUPID ignoring pion production with experiment, both plotted as a function of neutron incident energy.

Simulations using CUPID with pion production were compared with the same neutron data shown above and the details are given in [6]. An example of the comparisons is shown in Fig. 4 for 600 MeV neutrons. The fit at large energy depositions is excellent but there is still a significant difference between theory and experiment at low energy depositions which we attribute to elastic-scattering events. This difference between the measured total cross section and the calculated integral (CUPID with pion production) device cross section is compared to the total cross section in Fig. 5.

## III. Calculations for the CRRES PHA Detector

CUPID simulations were then carried out for the UV100 photodetector used in the CRRES PHA experiment for protons incident at 24 different energies in intervals of 10 MeV from 30 to 90 MeV and in intervals of 30 MeV from 90 to 600 MeV.

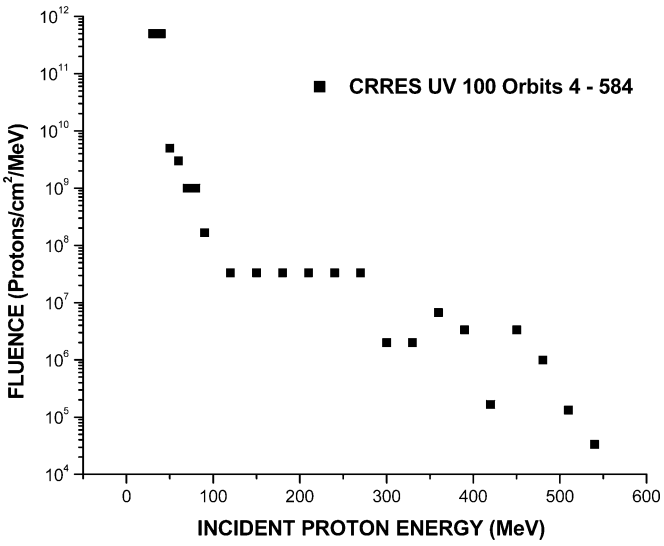


Fig. 6. Fluence of protons incident on the UV100 photodetector during orbits 4 through 584 as part of the CRRES PHA experiment. The fluence values were obtained from best fitting (1).

The dimensions of the cylindrical sensitive volume of the photodetector were 5 $\text{mm}^2$ in cross-sectional area and 26 $\mu$m in thickness. Since the probability of an elastic-scattering event depends on the cumulative proton track length in the detector, the total elastic-scattering-event cross sections were scaled for the UV100 from the values obtained from the Ortec detector by the ratio of the volumes. The energy deposition in elastic scattering was obtained from the energy transferred to the silicon nucleus. Since the elastic recoils are so short compared to the dimensions of the photodetector, they were assumed to lose all their energy within the detector. The number of events with energy deposition $\text{ED}_j$ to be expected in space can be obtained from the sum over the product of the fluence of protons with incident energy $E_i$, $F(E_i)$, and the cross section a proton with energy $E_i$ has for depositing energy $\text{ED}_j$.

$$N(\text{ED}_j) = \sum_i [F(E_i) \times \sigma_i(\text{ED}_j)] \tag{1}$$

where $E_i$ represents each of the 34 incident energies for which the combined CUPID and elastic scattering cross sections $\sigma(\text{ED}_j)$ for depositing energy $\text{ED}_j$ have been calculated. Equation (1) was inverted to obtain the fluence as a function of energy for the incident trapped protons. That is, the experimental CRRES PHA data for orbits 4 through 584 were substituted for each value of $N(\text{ED}_j)$ in (1) and the equation was best fitted to find the optimum values of the flux $F(E_i)$. The values of the fluence obtained are plotted as black squares as a function of $E_i$ in Fig. 6.

## IV. CRRES Orbit and the NASA Models

CRRES flew in a transfer orbit that had an 18 degree inclination with the equator, an apogee of 33 000 km, and a perigee of 350 km, giving it a period of about 9.62 hours. The PHA detector had shielding of 0.51 $\text{g/cm}^2$ Al on top due primarily to the Microelectronics Package Experiment cover and an estimated 20 $\text{g/cm}^2$ Al on the sides and bottom. During the flight there were

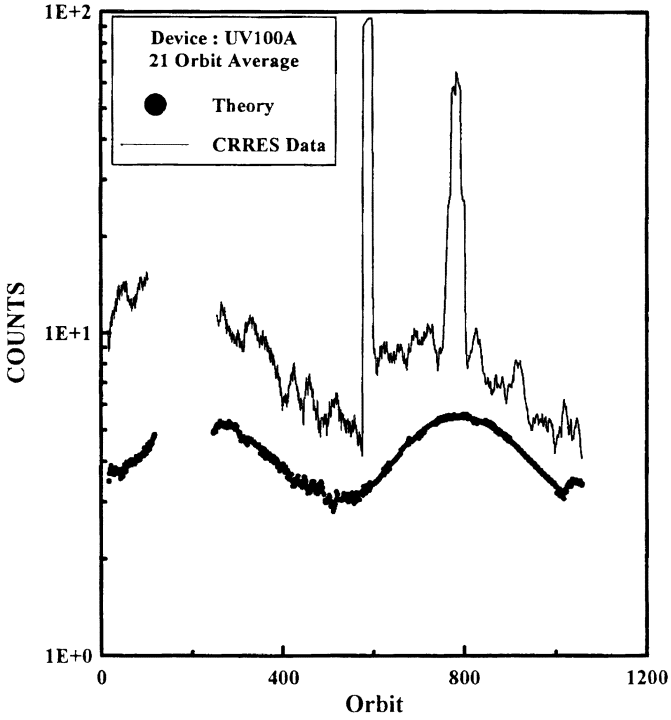


Fig. 7. CRRES PHA counts of events with energy depositions between 20 and 60 MeV plotted as a running 21 orbit average versus orbit number.

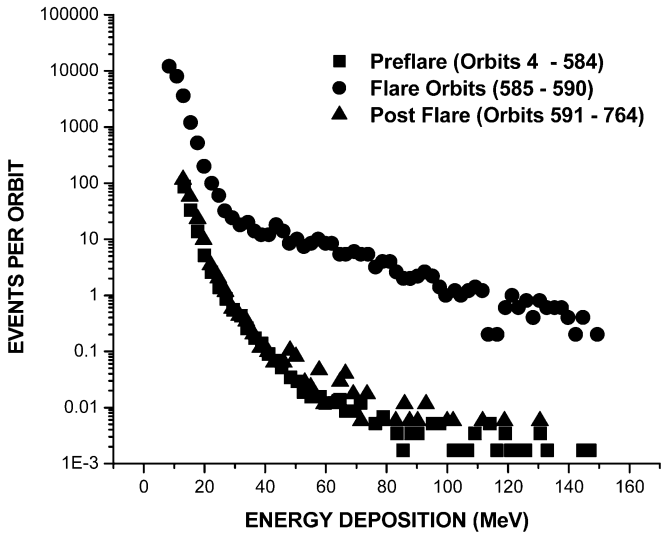


Fig. 8. Comparison of the energy-deposition spectra measured in the UV100 detector before the first SPE (orbits 4–584), during the SPE (orbits 585–590) and after the SPE (orbits 591–764).

two significant solar particle events (SPE) as shown in Fig. 7 which plots the number of events with energy depositions between 20 and 60 MeV as a function of orbit using a running 21 orbit average. The first SPE occurred during orbit 585 and lasted until orbit 590, and it was rich with particles with high atomic numbers (Z). The second SPE was of lower intensity and was composed entirely of protons.

We compare the energy deposition spectra obtained for before the first SPE with the data obtained during the SPE and after the SPE in Fig. 8. After the SPE, the radiation belts are

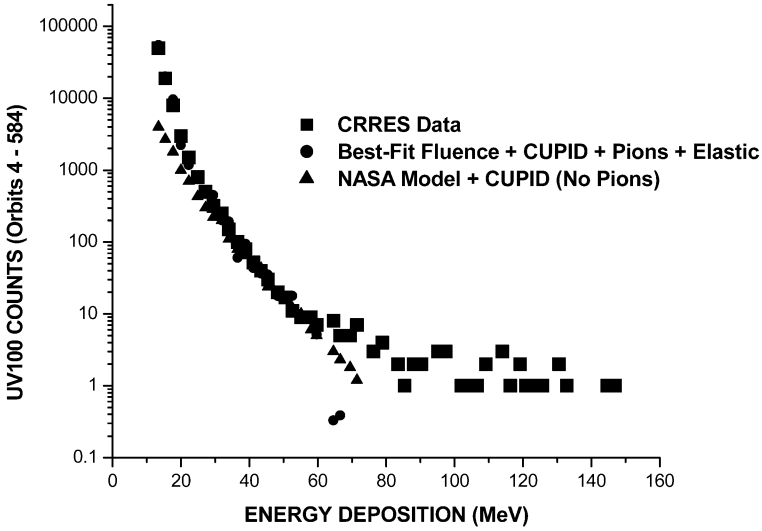


Fig. 9. Differential number of events in which energy $E$ is deposited within the sensitive volume of the UV100 photodetector. The squares represent CRRES PHA measurements obtained during orbits 4 through 584. Events above 60 MeV are due to cosmic-ray hits while the spacecraft was outside the proton belts and to a lesser extent inside the belts. The circles represent calculations carried out using CUPID with corrections for pion production and contributions from elastic scattering. These were obtained from (1) using the "best fit" values of the fluence determined from comparison with the integral spectrum given below. The triangles represent earlier calculations of Reed *et al.* [2] using the original version of CUPID and the fluence values calculated from AP-8 and USAF B–L coordinates.

known to have undergone significant changes including the temporary appearance of a third radiation belt that lasted until the CRRES experiment was completed. However, we see no important differences between the energy-deposition spectra obtained "before" and "after" the first event despite the fact that the "after" data includes the contribution from the second SPE. However, the spectra obtained during the five orbits of the first SPE are quite different from both "before" and "after." While the low-energy-deposition regions are similar in shape, the SPE data has considerably more high-energy-deposition events per orbit than "before" and "after." This could be due to a much higher proportion of high-energy protons in the SPE or the presence of high-Z particles. Since memory devices known to be sensitive to high-energy protons were on the other side of the circuit board and did not experience a significant increase in SEUs, we conclude that the flare had a significant number of low-energy high-Z nuclei. For comparison to the NASA models in the next paragraphs, we restrict our analysis to the PHA data obtained before the first SPE.

The differential energy-deposition spectrum for orbits 4 through 584 (before the first SPE) is shown in Fig. 9. The data shown are limited to that obtained during segments of the orbits that were within the inner radiation belt (the black squares represent experimental data). From Fig. 3, we know that the maximum energy deposition from proton interactions is about 100 MeV. From comparison with segments of the orbits that lie outside the proton belts and are dominated by cosmic rays, we find that these are generated by direct traversals by cosmic rays which are known to also penetrate the proton belts.

The CUPID simulations with pion production have shown excellent agreement with experimental data at accelerators, and the codes show all proton events should have energy depositions below 60 MeV as shown in Fig. 9. The PHA data above 60 MeV was, therefore, removed as being due to cosmic-ray

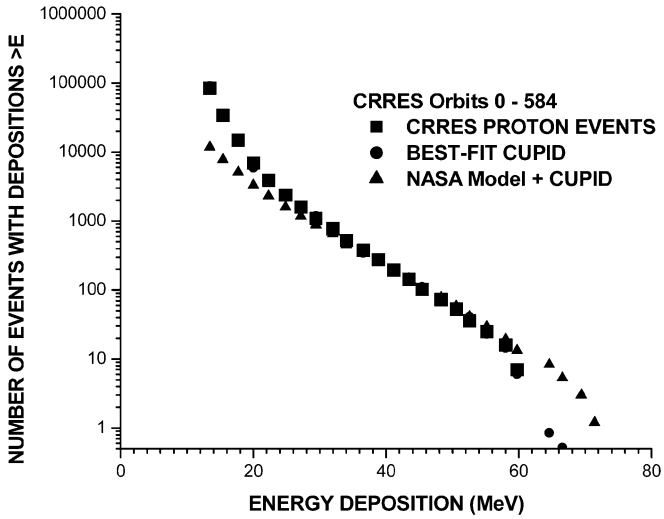


Fig. 10. Comparison with theory of the integral spectrum measured with the PHA instrument during orbits 4 through 584 on the CRRES satellite. Black squares are the experimental data. The circles are the spectum calculated using CUPID corrected for pion production and elastic scattering with the fluence values obtained as a "best fit" using (1). The triangles are the calculations of Reed *et al.* [2] for the orbits using the original CUPID and the fluence values calculated using the AP-8 model with the USAF B–L coordinates.

events, and the remaining data was plotted as an integral spectrum in Fig. 10. The "best fit" analysis using (1) described above was then performed to obtain the fluence of protons plotted in Fig. 6. The resulting "best fit" to the integral spectrum is shown as squares in Fig. 10. The triangles represent earlier calculations of Reed *et al.* [2] based on the original version of CUPID and the fluence values calculated directly from the AP8 model using the U.S. Air Force (USAF) B–L coordinates. The fit is good for both models at large energies, but the "best fit" model provides much better agreement at low-energy depositions for both the integral and differential spectra. However, since this agreement

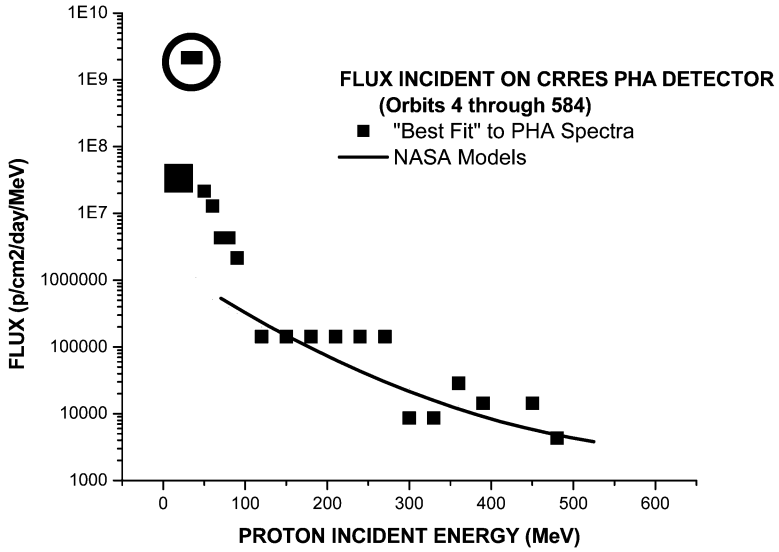


Fig. 11. Comparison of the average "best fit" flux of protons incident on the CRRES PHA experiment during orbits 4 through 584. The squares are the results of the best fit" to the PHA measurements. The solid curve represents the predictions of AP-8 using the USAF B–L coordinates. The agreement is excellent at high incident energies and reasonable between 50 and 100 MeV. The two lowest data points (30 and 40 MeV) are not in agreement with the model. However, these two data points are dominated by energy depositions between 13 and 20 MeV. Energy depositions above 13 MeV can be generated by protons entering the detector at grazing angles with at incident energies between 20 and 25 MeV. A flux of 20–25 Mev protons given by the large square in the figure would be sufficient to generate the two encircled data points.

was obtained with the "best fit" fluence values, there may still be a contribution due to grazing hits by low-energy protons.

The "best fit" fluence values were converted to flux by dividing the fluence by the product of the number of orbits (580), the time per orbit (9.62 hours/24 hours per day), and the number of MeV between data points (10 or 30). The results are plotted as squares versus incident energy in Fig. 11. The fluence generated by AP-8 and the USAF B–L coordinates are plotted for comparison. The fit is quite good for large incident energies, but very bad for the lowest two incident energies (30 and 40 MeV) and off by a factor of five at 50 MeV. These two data points are dominated by energy depositions between 13 and 20 MeV. However, depositions in that range do not require nuclear reactions. A proton incident on the detector at grazing angles with incident energies between 20 and 25 MeV can deposit at least 13 MeV by direct ionization. Protons in this energy range were not included in the simulations because they would not be able to deposit 13 MeV through nuclear reactions. Based on solid angle calculations, the flux of 20–25 MeV protons given by the large square in Fig. 11 would be sufficient when run through the simulation codes to generate the first two data points (circled). That fluence of 20–25 MeV particles is seen in the figure to be consistent with the fluence at higher incident energies. If we restricted the analysis to energy depositions above 20 MeV, the method could be used to generate the incident proton fluence with reasonable accuracy. The AP-8 model [9] combined with CUPID was shown to be accurate within a factor of two for a number of SEU measurements on CRRES as well as the PHA experiment [2]. In general, it is believed to be accurate within a factor of two. General inversion techniques using (1) and the PHA data sets do not provide a unique solution. However, relying on the known sharp fall-off in fluence with incident energy appears to provide reasonable agreement with the NASA models.

## V. Summary and Conclusion

The CRRES PHA data were used to generate the trapped proton flux in the inner radiation belt as a function of incident energy. The agreement is excellent above 100 MeV and within a factor of five above 50 MeV. The limits on large energy depositions imposed by pion production allowed for separating the contributions from cosmic rays with atomic number $\gg 1$. The very high event rate observed at low-energy depositions were due to low-energy protons (20–25 MeV) arriving at the detector at grazing incidence. There was a dramatic difference between the shape of the measured spectrum during the solar particle event that arrived during orbits 585–590 and the measurements obtained before the solar event and after. The anomalous number of high energy depositions could not be explained by a high fluence of high-energy protons because no increase in SEUs were observed during the SPE in proton–SEU-sensitive memories mounted on the backside of the circuit board.

The contribution from low-energy protons arriving at grazing incidence can be greatly reduced if the single sensitive volume of the photodetector is replaced with an array of small microvolumes connected in parallel. Sufficient spacing between microvolumes will reduce the chance of a single particle depositing a significant fraction of its energy within the array.

## References

[1] D. R. Roth, P. J. McNulty, W. J. Beauvais, R. A. Reed, and E. G. Stassinopoulos, "Solid-state microdosimeter for radiation monitoring in spacecraft and avionics," *IEEE Trans. Nucl. Sci.*, vol. 41, pp. 2118–2124, Dec. 1994.

[2] R. A. Reed, P. J. McNulty, W. J. Beauvais, W. G. Abdel-Kader, E. G. Stassinopoulos, and J. C. L. Barth, "A simple algorithm for predicting proton SEE rates in space compared to the rates in space measured on the CRRES satellite," *IEEE Trans. Nucl. Sci.*, vol. 41, pp. 2389–2395, Dec. 1994.

[3] G. E. Farrell, P. J. McNulty, and W. G. Abdel-Kader, "Microdosimetric analysis of proton-induced reactions in silicon and gallium arsenide," *IEEE Trans. Nucl. Sci.*, vol. NS-31, pp. 1073–1077, Dec. 1984.

[4] J. D. Kinnison, R. H. Maurer, D. R. Roth, and R. C. Haight, "High-energy neutron spectroscopy with thick silicon detectors," *Radiat. Res.*, vol. 139, pp. 154–160, 2003.

[5] P. W. Lisowski, C. D. Bowman, G. J. Russell, and S. A. Wender, "The los alamos national laboratory spallation neutron sources," *Nucl. Sci. Eng.*, vol. 106, pp. 208–208, 1990.

[6] J. D. Kinnison, R. H. Maurer, D. R. Roth, P. J. McNulty, and W. G. Abdel-Kader, "Neutron-induced pion production in silicon-based circuits," *IEEE Trans. Nucl. Sci.*, vol. 50, pp. 2251–2255, Dec. 2003.

[7] E. Segre, *Nuclei and Particles: An Introduction to Nuclear and Subnuclear Physics*, 2nd ed., W.A. Benjamin, Ed. New York, 1965.

[8] W. E. Burcham, *Nuclear Physics: An Introduction*. London, U.K.: Longman Group, Ltd., 1963.

[9] S. L. Huston, "Space Environments and Ffects: Trapped Proton Model,", NASA/CR-2002-211 784.